Maximum isotope accumulation in the retrosplenial cortex during amnesia attack and its temporal change suggest cortical spreading depression as a pathophysiology of patients with transient global amnesia

Short title: SPECT analysis of TGA

Yoshio Watanabe,[1*] Akira Taniguchi,[2] Hidekazu Tomimoto[2]

[1]Bethany Medical Neurological Clinic, 5-47-7, Toyogaoka, Tsu city, Mie, 514-0061, Japan

[2]Department of Neurology, Mie University School of Medicine, Edobashi, Tsu city, Mie, 514-8507, Japan

Yoshio Watanabe: ORCID: 0000-0001-5015-2502; E-mail: 07y.watanabe09@gmail.com

Akira Taniguchi: E-mail: a2005t@clin.medic.mie-u.ac.jp

Hidekazu Tomimoto: E-mail: tomimoto@clin.medic.mie-u.ac.jp

*Corresponding author: Yoshio Watanabe

Bethany Medical Neurological Clinic, 5-7-47, Toyogaoka, Tsu city, Mie, 514-0061, Japan

Tel.: +81-59-230-7373

Fax.: +81-59-230-7374

E-mail: 07y.watanabe09@gmail.com

Acknowledgements: The authors thank Dr. Shigeki Kuzuhara, Dr. Yugo Narita, Dr. Kiyomi Odachi, and Dr. Kaname Matsumura for their advice on the neurological diagnosis of TGA; Shigeki Tsuboi, Shigeru Aoki, and staff members at the Radiology Unit of Matsusaka Central General Hospital (M Hospital) for their assistance with SPECT and image processing for all patients in the present study; and Tetsuya Nishida, the scientific supervisor at Nihon MediPhysics Co., Ltd., for his advice on the interpretation of data from 3D-SSP analyses. We would also like to thank Medical English Service (https://www.med-english.com) for English language editing.

Conflict of interests

We declare no conflicts of interest associated with this manuscript.

Data Availability Statement

Data is available from the authors upon request.

Funding Statement

This research did not receive any specific grant from funding agencies in the public, commercial, or not-for-profit sectors.

Abstract

Transient global amnesia (TGA) is a clinical syndrome that is characterized by the sudden onset of anterograde amnesia and a less prominent impairment in retrograde memory lasting up to 24 h. Although several etiologies have been proposed, including migraine, epilepsy, ischemia, venous congestion, and glutamate toxicity, none sufficiently explain the disorder in its entirety. We retrospectively investigated images obtained using single-photon emission computed tomography (SPECT), performed with ^{99m}technetium hexamethylpropyleneamine oxime, from 11 patients with TGA divided into the following groups based on the timing of SPECT: during TGA (n = 2, Group 1), at the start of the attenuation of memory impairments (n = 2, Group 2), and after TGA (n = 7, Group 3). Regional isotope accumulation was examined using a three-dimensional stereotactic surface projection (3D-SSP) analysis. After calculating the mathematical product of the mean severity and extent ratio, unique comparable bar graphs were prepared with respect to Brodmann's areas (B). Increases in isotope accumulation were the largest in the retrosplenial cortex (B29, B30), posterior cingulate cortex (B23, B31), and precuneus (B7) in Groups 1 and 2, whereas decreases were noted in the same regions in Group 3. This is the first study to identify cerebral sites and describe changes consistent with the completion of amnesia as a symptom using an image analysis, such as a 3D-SSP analysis. We consider cortical spreading depression (CSD) to be the etiology of TGA based on maximum isotope accumulation in the above sites and a literature review on CSD.

Keywords: single-photon emission computed tomography; three-dimensional stereotactic surface projections; transient global amnesia; cortical spreading depolarization; retrosplenial cortex; posterior cingulate cortex; Brodmann area 7

1. Introduction

Transient global amnesia (TGA) was initially described by Benon.[1] However, a consensus has not yet been reached on its etiology or pathogenesis.[2,3] TGA is a temporal and functional clinical syndrome that is characterized by the sudden onset of anterograde amnesia and a milder retrograde episodic long-term memory distubance,[4] which has contributed to the delay in clarifying its pathophysiology and the difficulties associated with diagnostic imaging.

Although several etiologies have been proposed, including migraine, epilepsy, ischemia, venous congestion, and glutamate toxicity;[5-7] none sufficiently explain the etiology of TGA. Olesen and Jørgensen[8] suggested cortical spreading depression (CSD) as an underlying etiology for TGA, and this is supported by accumulating evidence from an increasing number of studies.[9-15] CSD has been detected in the human brain.[16-18] Corresponding findings on hemodynamic and morphological changes in TGA and CSD have been separately obtained; however, similarities between TGA and CSD have yet to be systematically examined.[19]

Although we previously proposed a causal relationship between TGA and CSD, our study involved a small number of patients. Since the latest single photon emission computed tomography (SPECT) system was introduced in 1992 in Matsusaka Central General Hospital (M Hospital) to which we belong, the 1st session of SPECT has been performed on patients with TGA during an attack and a few hours after the completion of the attack. In addition, the 2nd session of SPECT has been conducted on the same patients after a few months of rehabilitation after the completion of the attack. The annual number of TGA patients with these attacks in M Hospital is only approximately 10, and these attacks disappear a few hours

after consultation. Therefore, it is extremely difficult to accurately make a diagnosis and promptly perform SPECT during this short timeframe. Furthermore, even after the disappearance of amnesia, the low accumulation of isotopes in the medial temporal lobe persists for a long time. Many studies reported that the phase after attack completion corresponded to the acute stage of TGA attacks, which has confused investigators specializing in TGA.

A rapid change in isotope accumulation was previously observed before and after the disappearance of amnesia attacks even though the number of patients examined was small (n=4). Although many studies have discussed the etiology of TGA using SPECT or positron emission tomography (PET), none have reported the site or described cerebral changes on imaging in the acute stage using a three-dimensional stereotactic surface projection (3D-SSP) analysis.

Even though the rat brain is smaller and less complex than the human brain, research has shown that the two are remarkably similar in structure and function and many aspects are anatomically similar between human and rat brains.[20] Therefore, if CSD does not propagate to Rsc/Pcc/B7 in the rat brain, a similar finding may also be obtained in the human brain.

We speculated that the mechanisms underlying retrosplenial cortex (Rsc)/posterior cingulate cortex (Pcc)/precuneus (B7)-specific changes in isotope accumulation may provide insights into the etiology of TGA. We also discussed the etiology of TGA with reference to the literature.

2. Materials and Methods

2.1 Patients

This retrospective study included 11 patients with TGA (Table 1) who presented to M Hospital as outpatients. Between 1993 and 2016, 26 patients were diagnosed with TGA according to the criteria described by Caplan[21] and Hodges and Warlow.[22] Exclusion criteria included patients with neurological, psychiatric, or medical conditions and those with MRI findings indicating cerebrovascular disorders. A 1.0-T Shimazu MRI SMT-100X device was used with the automatic registration tool 2.03 (Toshiba, Tokyo, Japan) as imaging software. MRI did not include diffusion-weighted imaging sequences. Data were obtained from 11 patients who underwent ^{99m}technetium hexamethylpropyleneamine oxime (^{99m}Tc-HMPAO)SPECT and were categorized as follows: Patients 1 and 2, with TGA that continued after SPECT, were assigned to Group 1; Patients 3 and 4, with TGA that occurred during SPECT, but with no memory loss at the end of the examination, were assigned to Group 2; Patients 5– 11, with TGA that ended and who had stabilized before SPECT, were assigned to Group 3. The environment in which data were collected and processed using the gamma-camera remained consistent for all 11 patients and healthy control subjects. The data used to create the control database were obtained at the same hospital during the same period of time. Data were collected from all patients using the same device.

Table 1. Grouping of patients with transient global amnesia.

	Patients with TGA						
	Case	**Age**	**Sex**	**Circumstances at the time of TGA**	**Duration of seizure (h)**	**SPECT timing**	**Time between the start of TGA and SPECT (h)**
Group 1	1	66	M	In a meeting at the office	20	During TGA	5
	2	57	F	Cleaning at home	9	During TGA	6
Group 2	3	55	F	Conversing with family members	7	Around the time TGA concluded	6
	4	63	F	Cleaning at home	10	Around the time TGA concluded	9
Group 3	5	58	M	On a train on the way home	12	Immediately after TGA concluded	15
	6	54	M	Having a meal at home	12	5 h after TGA concluded	19
	7	60	M	Doing housework at home	7	10 h after TGA concluded	23
	8	69	F	Chatting with a friend	15	10 h after TGA concluded	28
	9	33	F	Working at a coffee shop	6	3 h after TGA concluded	30
	10	73	F	Doing office work	8	25 h after TGA concluded	28
	11	60	F	Doing office work	8	25 h after TGA concluded	28

2.2 Control group

SPECT data from 20 healthy subjects (age, 32–78 years; mean age, 60.1 ± 5.4 years; 65% female) were used as the control in the 3D-SSP analysis. The same camera and SPECT device were used in the analysis of all subjects. Healthy subjects had no history of neurological or psychiatric disorders.

2.3 SPECT study protocol

All subjects received 740 MBq (20 mCi) of ^{99m}Tc-HMPAO intravenously in the supine position on the scanning couch under standard resting conditions. The 3-head GCA-9300A SPECT system (Toshiba) was equipped with low-energy, ultra-high-resolution fan-beam collimators and a GMS-5500A/PI data processor (Toshiba). Data were acquired for 15 minutes, beginning 5 minutes after the administration of ^{99m}Tc-HMPAO. The distance of the collimators from the center of rotation was kept constant at 13.2 cm. Each detector was set to rotate continuously through 120° in 3 minutes, alternating in clockwise and counterclockwise directions. The triple-energy window method was used for scatter corrections. Images were reconstructed in a 128 × 128 matrix, with a pixel size of 1.72 mm, using a ramp filter with six attenuation corrections according to Chang's technique[23] after data were processed with a Butterworth filter with an order of 8 and cut-off of 0.12 cycles per pixel.

2.4 SPECT data analysis

Relative decreases or increases in the uptake of ^{99m}Tc-HMPAO were measured using 3D-SSP based on the original 3D-SSP program described by Minoshima et al.[24,25] This procedure was performed using NEUROSTAT (Nihon Medi-Physics Co., Ltd., Tokyo, Japan), which is interface software that anatomically transforms individual SPECT images to the standard brain according to the Talairach–Tournoux atlas.[26] Datasets were normalized to mean global activity.[27] Regional voxel data were compared with the normal database using NEUROSTAT, calculating the *z*-score [*z*-score = (normal values for the healthy group)/standard deviation for the healthy group] for each voxel of the cerebral surface. To quantitatively assess changes in regional cerebral blood flow, the mean *z*-scores for each lobe and gyrus levels were assessed using the stereotactic extraction estimation method.[28] 3D-SSP extracted 3D functional information from the gray matter using pixels preset to cover the whole brain surface after the brain image of each subject was transformed to the standard brain image through anatomical standardization. Normalization was performed by whole brain counting.

We investigated 78 regions bilaterally based on Brodmann's areas (B). In the original version of B, B1–B52 are categorized based on neuronal structures in the cerebral cortex stained in the postmortem brain.[29] A 3D-SSP analysis generally excludes B12–B16, B26, B27, B41, and B48–B52 because they are not visualized on the brain lateral projection surface. In the present study, the *z*-scores of B29, B33, and B35 were analyzed as reference values due to the small pixel count. The following procedures were performed to create graphs using the *z*-scores of all subjects.

Two graphs displaying relative decreases (d) and increases (i) in B(a) are shown on the left and right sides, respectively. We then created (−1) × dB (1–47) and iB (1−47) bar graphs for all regions. In the left (decrease) graph, (−1) × extent ratio × mean severity = (−1) × dB(a), and in the right (increase) graph, extent ratio × mean severit = iB(a).

Patient 1 underwent SPECT again 7 months after TGA, and the results obtained were used to calculate the same dB (1–47)* and iB (1–47)*. In the left (decrease) graph, (−1) × dB (1–47) − (−1) × dB (1–47)*. In the right (increase) graph, iB (1–47)–iB (1–47)*. This was used to derive the coefficient of variation, after which the same type of bar graph was created.

The present study was approved by the Ethics Standards Committee of M Hospital (Approval number: 201; Approval date: October 25, 2018). Since SPECT was performed 25 years ago, it was not feasible to obtain written consent from all patients. This study was compliant with ethical guidelines for clinical studies (Opt-out) on the M Hospital website (http://www.miekosei.or.jp/1_mch/pdf/optout/201811-9.pdf).

The present study included 11 patients with TGA (Table 1) who presented to M Hospital for the use of an opt-out methodology, which was based on the low risk and potential benefits of the adequate management of TGA in patients.

3. Results

The results of initial 3D-SPP for Patient 1, a 66-year-old male, are shown in Table 2. In the statistical maps analyzed by the 3D-SSP two-tail view for Patient 1 (Fig 1), relative increases in tracer uptake were observed in regions equivalent to the right Rsc/Pcc/B7, right posterior cortex, and part of the right anterior cingulate cortex. In addition, relative decreases in tracer

uptake were noted in the regions equivalent to the area of the medial side of the temporal lobe. In Patient 1, SPECT was performed 7 months after TGA (Fig 2). A bar graph created from the results of Patient 1 indicated (−1) × dB on the left (decrease) of the graph and iB on the right (increase) of the graph for all regions (Fig 3).

Bar graphs were based on data obtained from initial SPECT, second SPECT, and the coefficient of variation shown in the upper, middle, and lower rows, respectively. Initial SPECT showed maximum positive changes in B30, B5, and B7 as well as in B10 and B17, and negative changes in B20, B28, B34, B35, B36, B38, B24, B25, B29, and B23. A clear comparison was made by calculating the coefficient of variation, which indicated a maximum positive change in B30 and maximum negative change in B28. Highly positive iB values in B30, B23, B5, and B7 were observed in Groups 1 and 2 (Fig 4), but not in Group 3 (Fig 5). In the temporal lobe, maximum negative dB values were primarily noted in B28, B34, B35, B36, and B38 in Groups 1–3. Based on these results, changes in dB and iB values corresponding to clinical symptoms were only observed in Rsc/Pcc/B7 (Fig 6).

Table 2. Results of initial 3-dimensional stereotactic surface projections for Patient 1 (67-year-old male).

ROI (Lt / Rt)	total projection	During TGA				Seven months after the conclusion of TGA			
		Increase		Decrease		Increase		Decrease	
		extent ratio (%)	severity mean	extent ratio (%)	severity mean	extent ratio (%)	severity mean	extent ratio (%)	severity mean
Brodmann 20	233	0.9	0.61	99.1	3.74	7.3	0.31	92.7	2.48
Inferior temporal gyrus	233	0	0	100	2.18	24.5	1.42	75.5	1.54
Brodmann 21	229	4.4	0.43	95.6	2.63	31.9	0.62	68.1	1.53
Middle temporal gyrus	229	35.8	0.64	64.2	1.89	31.9	0.99	68.1	0.75
Brodmann 22	172	54.7	1.53	45.3	1.06	80.8	1.03	19.2	1.02
Superior temporal gyrus	172	73.3	1.25	26.7	0.96	52.9	0.99	47.1	1.26
Brodmann 23	95	25.3	2.22	74.7	2.7	25.3	0.88	74.7	2.53
Ventral posterior cingulate c.	95	26.3	2.14	73.7	3	12.6	0.99	87.4	1.79
Brodmann 24	223	1	0.32	99.1	2.46	0	0	100	2.14
Ventral anterior cingulate c.	223	3	0.29	97.3	2.14	2.7	0.22	97.3	2.09
Brodmann 25	116	0	0	100	4.37	0	0	100	3.77
Subgenual area	116	0	0	100	2.7	0	0	100	2.8
Brodmann 28	41	0	0	100	5.11	0	0	100	4.55
Ventral entorhinal cortex	41	0	0	100	3.69	0	0	100	4.03
Brodmann 29	42	9.5	0.45	90.5	3.44	0	0	100	4.1
Retrosplenial cortex	42	23.8	1.78	76.2	3.24	14.3	0.43	85.7	2.82
Brodmann 30	64	57.8	3.04	42.2	1.63	4.7	0.15	95.3	1.49
Subdivision of retrosplenial c.	64	78.1	3.29	21.9	2.03	18.8	0.24	81.3	0.98
Brodmann 31	150	48.7	2.05	51.3	1.52	68	1.65	32	1.36
Dorsal posterior cingulate c.	150	59.3	1.75	40.7	1.25	68	1.54	32	1.22
Brodmann 32	132	62.1	0.81	37.9	0.5	25	0.85	75	0.97
Dorsal anterior cingulate c	132	78.8	1.03	21.2	0.62	34	0.78	65.9	0.91

Brodmann 33	18	0	0	100	0.97	0	0	100	1.31
Part of anterior cingulate c.	18	0	0	100	1.37	0	0	100	1.79
Brodmann 34	31	0	0	100	4.64	0	0	100	3.62
Dorsal entorhinal cortex	31	0	0	100	3.04	0	0	100	2.97
Brodmann 35	35	0	0	100	4.57	0	0	100	4.21
Part of the perirhinal cortex	35	0	0	100	2.69	0	0	100	2.45
Brodmann 36	53	0	0	100	5.56	0	0	100	4.87
Part of the perirhinal cortex	53	0	0	100	3.02	0	0	100	3.4
Brodmann 37	104	46.2	0.81	53.8	1.75	48.1	1.03	51.9	0.9
Fusiform gyrus	104	43.3	1.29	56.7	0.92	74	1.45	26	0.64
Brodmann 38	129	0	0	100	3.47	0	0	100	3.57
Temporopolar area	129	0.8	0.17	99.2	2.22	0	0	100	3.58

Z-scores (mean severity for increases and decreases) and extent ratios (%) according to initial ^{99m}technetium hexamethylpropyleneamine oxime single-photon emission computed tomography with 3-dimensional stereotactic surface projections (3D-SSP) are indicated. Note that all regions are not presented above because

4. Discussion

We confirmed increases in the accumulation of 99mTc-HMPAO in Rsc/Pcc/B7 during attacks and decreases after the completion of attacks in patients with TGA. These changes cannot be

explained by posterior circulation strokes, transient epileptic amnesia, psychogenic amnesia, post-traumatic amnesia, or toxic/drug-related amnesia, which were previously reported as etiological factors for TGA.

Leão,[30] who initially identified CSD in the rat brain, demonstrated that a wave of depolarization spread throughout the cortex, except the Rsc. In rats, the terms “retrosplenial cortex” and “posterior cingulate cortex” are often used as synonyms, and the B29 and B30 areas of the rat brain may be the same as the B23, B29, B30, and B31 areas of the human brain. As demonstrated for the rat brain, if the wave of depolarization does not spread to these areas in the human brain, isotope accumulation during attacks in TGA patients may markedly differ between these and other areas. In the present study, we retrospectively examined patients and confirmed the above hypothesis. Our results support CSD being an etiological factor for TGA.

Regarding increases in isotope accumulation in the precuneus, Brent et al. identified the posterior cingulate, precuneal, and retrosplenial cortices as critical nodes in the neural network of consciousness[31]. Furthermore, these regions have the highest level of cortical glucose metabolism and cytochrome c oxidase activity. It currently remains unclear whether CSD involves B7; however, one of the reasons for an increase in isotope accumulation may be the presence of a common function between Rsc/Pcc and the precuneus.

If CSD propagates to Rsc/Pcc in the human brain, it is challenging to explain these changes in Rsc/Pcc based on the many other theories on the etiology of TGA.[32]

A brief explanation of the methods used to analyze and interpret the results of SPECT is provided below.

(1) Validity of the coefficient of variation: The analysis using the coefficient of variation was a trial to elucidate slight changes in isotope accumulation on SPECT. Patient 1 showed continuous low isotope accumulation on the medial side of the temporal lobe 7 months after TGA. This change was observed on SPECT after the patient recovered from TGA. This is evidence of the predominant cause of TGA and that variations between the first and second sessions of SPECT facilitated attempts to elucidate the etiology of TGA. By subtracting the dB and iB values of second SPECT from those of first SPECT, the regions that underwent major changes from normal at the time of the latter became clearer.

(2) Comparisons of recent studies using functional MRI and statistical parametric mapping. Jang et al.[33] reported that among 22 cases of TGA examined using a high-resolution SPECT device, cerebral perfusion significantly decreased at left B7 ($P < 0.001$, uncorrected). These cases would have been assigned to Group 3 in the present study. Detailed image analyses were performed by Kim et al.[34] (6 cases) and Chung et al.[35] (7 cases), and their cases would also have been assigned to Group 3 in the present study, allowing for comparisons with our patients. Therefore, the pathogenesis of TGA may be examined based on the changes in isotope accumulation that occur during TGA rather than after the conclusion of an attack.

(3) B29 and B30 in Patient 1 showed the greatest isotope accumulation during a TGA attack. In contrast, B20, B27, B28, B35, and B37, which correspond to the medial temporal lobe, showed the lowest isotope accumulation. These areas are almost adjacent to B29 and B30, and isotope accumulation in B29 and B30 is affected by B20, B27, B28, B35, and B37 due to the partial-volume effect. Therefore, isotope accumulation may be higher than the 3DSSP-displayed Z scores for B29 and B30 in Case 1.

(4) Consistency with previous cases of TGA assuming that CSD is the etiology of TGA. If

CSD is an etiology for TGA, the issue of consistency with previous cases of TGA persists.[3] According to Olesen and Jørgensen,[8] glutamate, which is present in large amounts in the hippocampus, experimentally elicited CSD, which may be triggered by strong emotional and physical events. Therefore, TGA appears to occur as a result of CSD that is a secondary effect of these stressors.

(5) The 11 patients in the present study did not undergo diffusion-weighted MRI; therefore, patients with transient ischemic attacks (TIA) may have been included. The present results revealed an increase in the accumulation of nuclides in Rsc/Pcc/B7 during an attack. TIA may occur in ischemic diseases, with the accumulation of nuclides decreasing during attacks. Rsc/Pcc/B7 are perfused by the terminal branches of the anterior and posterior cerebral arteries, and when boundaries are unclear, it is not a vascular lesion, thereby confirming that the episode is not TIA.

5. Conclusions

SPECT on patients with TGA revealed increases in isotope accumulation in Rsc/Pcc/B7, which subsequently decreased after the conclusion of the episode. If CSD is not transmitted to Rsc/Pcc/B7 in the human brain, similar to the rat brain, the present results support CSD as an etiology of TGA and also provide novel insights into its etiology.

References

1. Benon R. Les ictus amnésiques dans les démences ‘organiques’. Ann Méd Psychol. 1909;67: 207-219.

2. Bartsch T, Deuschl G. Transient global amnesia: functional anatomy and clinical implications. Lancet Neurol. 2010;9: 205-214. doi: 10.1016/S1474-4422(09)70344-70348.

3. Arena JE, Rabinstein AA. Transient global amnesia. Mayo Clin Proc. 2015;90: 264-272. doi: 10.1016/j.mayocp.2014.12.001.

4. Spiegel DR, Smith J, Wade RR, et al. Transient global amnesia: current perspectives. Neuropsychiatr Dis Treat. 2017;13:2691-2703. doi: 10.2147/NDT.S130710.

5. Romero JR, Mercado M, Beiser AS, et al. Transient global amnesia and neurological events: the Framingham Heart Study. Sec. Stroke. 2013;4:47. doi: /10.3389/fneur.2013.00047.

6. Ogawa K, Suzuki Y, Akimoto T, et al. Relationship between cytotoxicity in the hippocampus and an abnormal high intensity area on the diffusion-weighted images of three patients with transient global amnesia. Intern. Med. 2018;57: 2631–2639. doi: 10.2169/internalmedicine.0251-17

7. Han K, Hu HH, Chao AC, et al. Transient global amnesia linked to impairment of brain venous drainage: An ultrasound investigation. Front Neurol. 2019;10:67. doi: 10.3389/fneur.2019.00067. eCollection 2019.

8. Olesen J, Jørgensen MB. Leao’s spreading depression in the hippocampus explains transient global amnesia. A hypothesis. Acta Neurol. Scand. 1986;73: 219-220. doi: 10.1111/j.1600-0404.1986.tb03267.x.

9. MeloTP, Ferro JM, Ferro H. Transient global amnesia. A case control study. Brain. 1992;115: 261-270. doi: 10.1093/brain/115.1.261.

10. Zorzon M, Antonutti L, Masè G, et al. Transient global amnesia and transient ischemic attack. Natural history, vascular risk factors, and associated conditions. Stroke. 1995;26: 1536-1542. doi: 10.1161/01.str.26.9.1536.

11. Strupp M, Brüning R, Wu RH, et al. Diffusion-weighted MRI in transient global amnesia: elevated signal intensity in the left mesial temporal lobe in 7 of 10 patients. Ann Neurol. 1998;43: 164-170. doi: 10.1002/ana.410430206.

12. Fisher M, Albers GW. Applications of diffusion-perfusion magnetic resonance imaging in acute ischemic stroke. Neurology. 1999;52: 1750-1756. doi: 10.1212/wnl.52.9.1750.

13. Quinette P, Guillery-Girard B, Dayan J, et al. What does transient global amnesia really mean? Review of the literature and thorough study of 142 cases. Brain. 2006; 129: 1640–1658. doi: 10.1093/brain/awl105.

14. Spiegel DR, Smith J, Wade RR, et al. Transient global amnesia: current perspectives. Neuropsychiatr Dis Treat. 2017;13:2691-2703. doi: 10.2147/NDT.S130710.

15. Montagna P, Cerullo A, Cortelli P. Transient global amnesia occurring as migraine aura. J Headache Pain. 2002;1:57–59. https://thejournalofheadacheandpain.biomedcentral.com/articles/10.1007/s101940050012

16. Strong AJ, Fabricius M, Boutelle MG, et al. Spreading and synchronous depressions of cortical activity in acutely injured human brain. Stroke. 2002;33: 2738-2743. doi: 10.1161/01.str.0000043073.69602.09.

17. Fabricius M, Fuhr S, Bhatia R, et al. Cortical spreading depression and peri-infarct depolarization in acutely injured human cerebral cortex. Brain. 2006;129: 778-790. doi: 10.1093/brain/awh716.

18. Dohmen C, Sakowitz OW, Fabricius M, et al. Spreading depolarizations occur in human ischemic stroke with high incidence. Ann Neurol. 2008;63: 720-728. doi: 10.1002/ana.21390.

19. Ding X, Peng D. Transient global amnesia: an electrophysiological disorder based on cortical spreading depression-transient global amnesia model. Front Hum Neurosci. 2020; 14:602496. doi: 10.3389/fnhum.2020.602496.

20. Vermaercke B. Rats Can Be Smarter Than People. Harvard Business Review. Magazine (January–February 2015) https://hbr.org/2015/01/rats-can-be-smarter-than-people

21. Caplan LR. Transient global amnesia: criteria and classification. Neurology. 1986;36: 441-442. doi: 10.1212/WNL.36.3.441.

22. Hodges JR, Warlow CP. The etiology of transient global amnesia: a case control study of 114 cases with prospective follow-up. Brain. 1990;113: 639-657. doi: 10.1093/brain/113.3.639.

23. Chang LT. A method for attenuation correction in radionuclide computed tomography.

IEEE Trans Nucl Sci. 1978;25: 638-643. doi: 10.1109/TNS.1978.4329385.

24. Minoshima S, Frey KA, Koeppe RA, Foster NL, Kuhl DE. A diagnostic approach in Alzheimer's disease using three-dimensional stereotactic surface projections of fluorine-18-
FDG PET. J Nucl Med. 1995;36: 1238-1248.

25. Minoshima S, Giordani B, Berent S, et al. Metabolic reduction in the posterior cingulate cortex in very early Alzheimer's disease. Ann Neurol. 1997;42: 85-94. doi:
10.1002/ana.410420114.

26. Talairach J, Tournoux P. Co-planar stereotaxic atlas of the human brain. 3-Dimensional proportional system: an approach to cerebral imaging. 1st ed. New York: Thieme Medical Publishers; 1988. pp. 9-18.

27. Minoshima S, Koeppe RA, Frey KA, Kuhl DE. Anatomic standardization: linear scaling and nonlinear warping of functional brain images. J Nucl Med. 1994;35: 1528-1537.

28. Mizumura S, Kumita S, Cho K, et al. Development of quantitative analysis method for stereotactic brain image: assessment of reduced accumulation in extent and severity using anatomical segmentation. Ann Nucl Med. 2003;17: 289-295. doi: 10.1007/BF02988523.

29. Laurence J. Brodmann's localisation in the cerebral cortex. 3rd ed. New York: Springer;
2005. pp. 105-126.

30. Leão AAP. Spreading depression of activity in the cerebral cortex. J Neurophysiol.
1944;7: 359-390. doi: 10.1152/jn.1944.7.6.359.

31. Vogt BA, Laureys S. Posterior cingulate, precuneal and retrosplenial cortices: cytology and components of the neural network correlates of consciousness. Prog Brain Res.
2005;150:205-17. doi: 10.1016/S0079-6123(05)50015-3.

32. Quinette P, Guillery-Girard B, Dayan J, et al. What does transient global amnesia really mean? Review of the literature and thorough study of 142 cases. Brain. 2006;129: 1640-1658. doi: 10.1093/brain/awl105.

33. Jang JW, Park YH, Park SY. Longitudinal cerebral perfusion change in transient global amnesia related to left posterior medial network disruption. PLoS One. 2015;10: e0145658. doi: 10.1371/journal.pone.0145658.

34. Kim BS, Cho SS, Choi JY, Kim YH. Transient global amnesia: a study with Tc-99m ECD

SPECT shortly after symptom onset and after recovery. Diagn Interv Radiol. 2016;22: 476-480. doi: 10.5152/dir.2016.15487.

35. Chung YA, Jeong J, Yang DW, et al. A Tc-99m SPECT study of regional cerebral blood flow in patients with transient global amnesia. Neuroimage. 2009;47: 50-55. doi: 10.1016/j.neuroimage.2008.11.011.

Figure legends

Fig 1. Statistical maps in Patient 1 analyzed by three-dimensional stereotactic surface projection two-tail views for $^{99\,m}$technetium hexamethylpropyleneamine oxime single-photon emission computed tomography performed during transient global amnesia. The color of the outer counter corresponds to a *z*-score of 7. A relative increase in tracer uptake (*z*-score, 1–3) was observed in the area corresponding to the right retrosplenial cortex, right posterior cingulate cortex, right Brodmann area 7, and right posterior cortex. A relative decrease in tracer uptake (*z*-score, 1–3) was noted in the left temporal lobe.

Fig.1

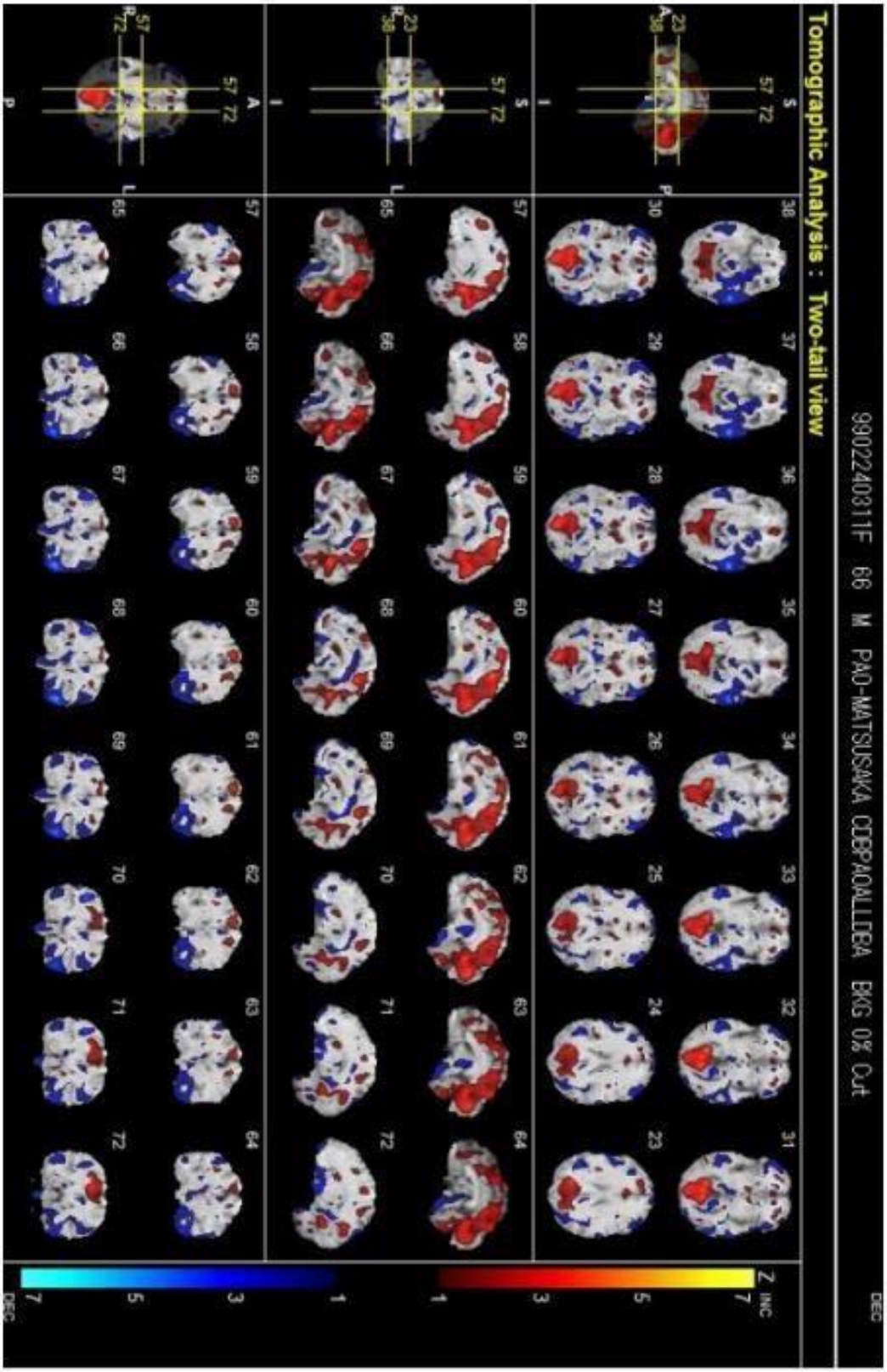
9902240311F 66 M PAD-MATSUSAKA COEPAOALLEEA BKG 0% Cut
Tomographic Analysis : Two-tail view
Z INC
DEC

Fig 2. Two-tail view of a single-photon emission computed tomography image in Patient 1 acquired 7 months after transient global amnesia. In comparisons with Fig 1, an overall decrease was observed in the relative levels of tracer uptake (z-score, ≤ 3).

Fig.2

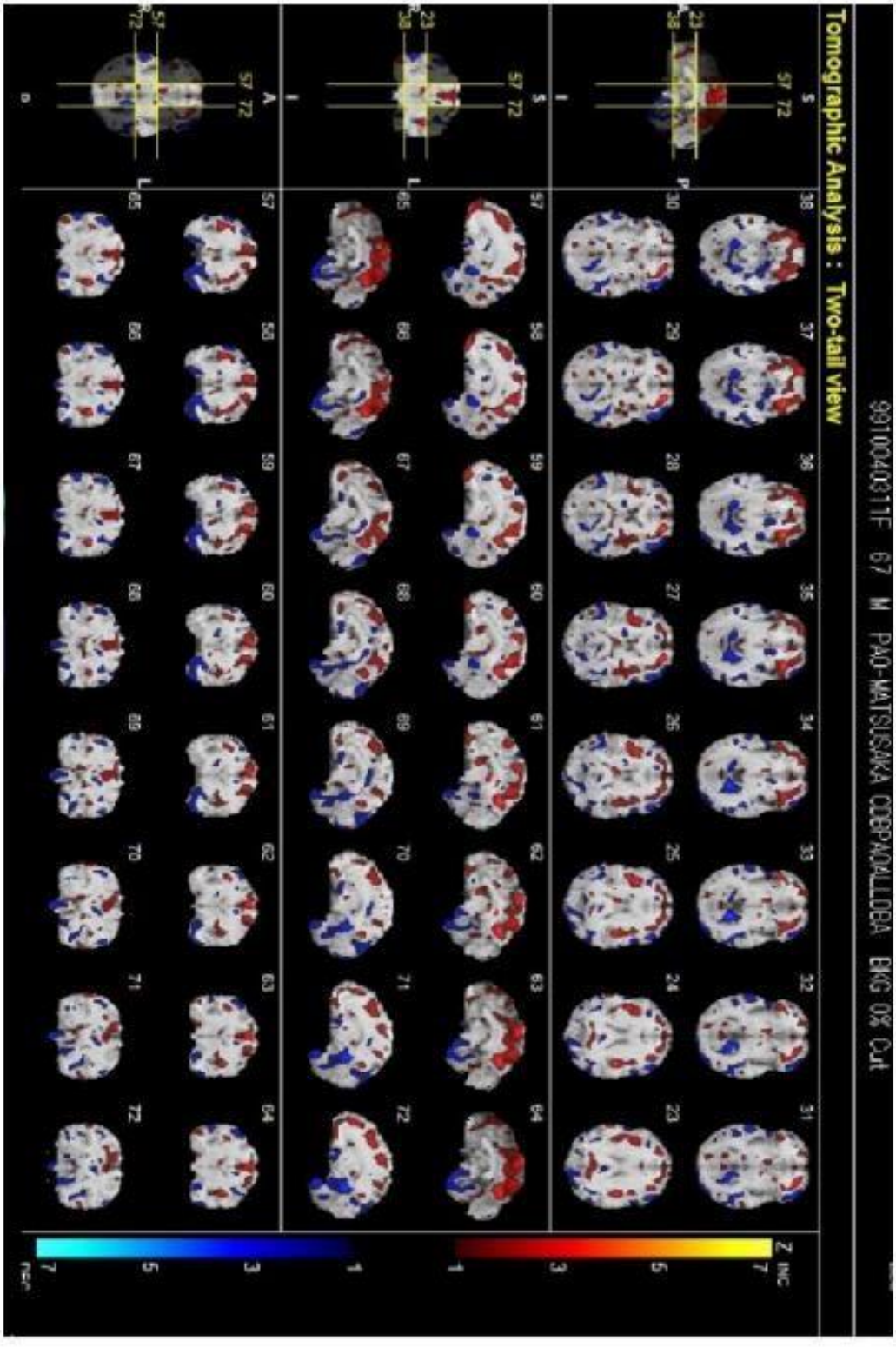
9910040311F 67 M PAD-MATSUSAKA CDP/ADALLDEA BKG 0% Cut
Tomographic Analysis : Two-tail view
Z INC
neg

Fig 3. Bar graphs showing initial single-photon emission computed tomography (SPECT), second SPECT, and the coefficient of variation in Patient 1 on the upper, middle, and lower rows, respectively. Sites at which iB and dB clearly had high values are shown in red and blue, respectively. In initial SPECT, visible increases {dB (1) ≥ 2} were observed in B10, B30, B5, B7, and B17. These increases in B30 and B7 disappeared in second SPECT. An investigation of the coefficient of variation indicated that B30 showed the maximum positive change.

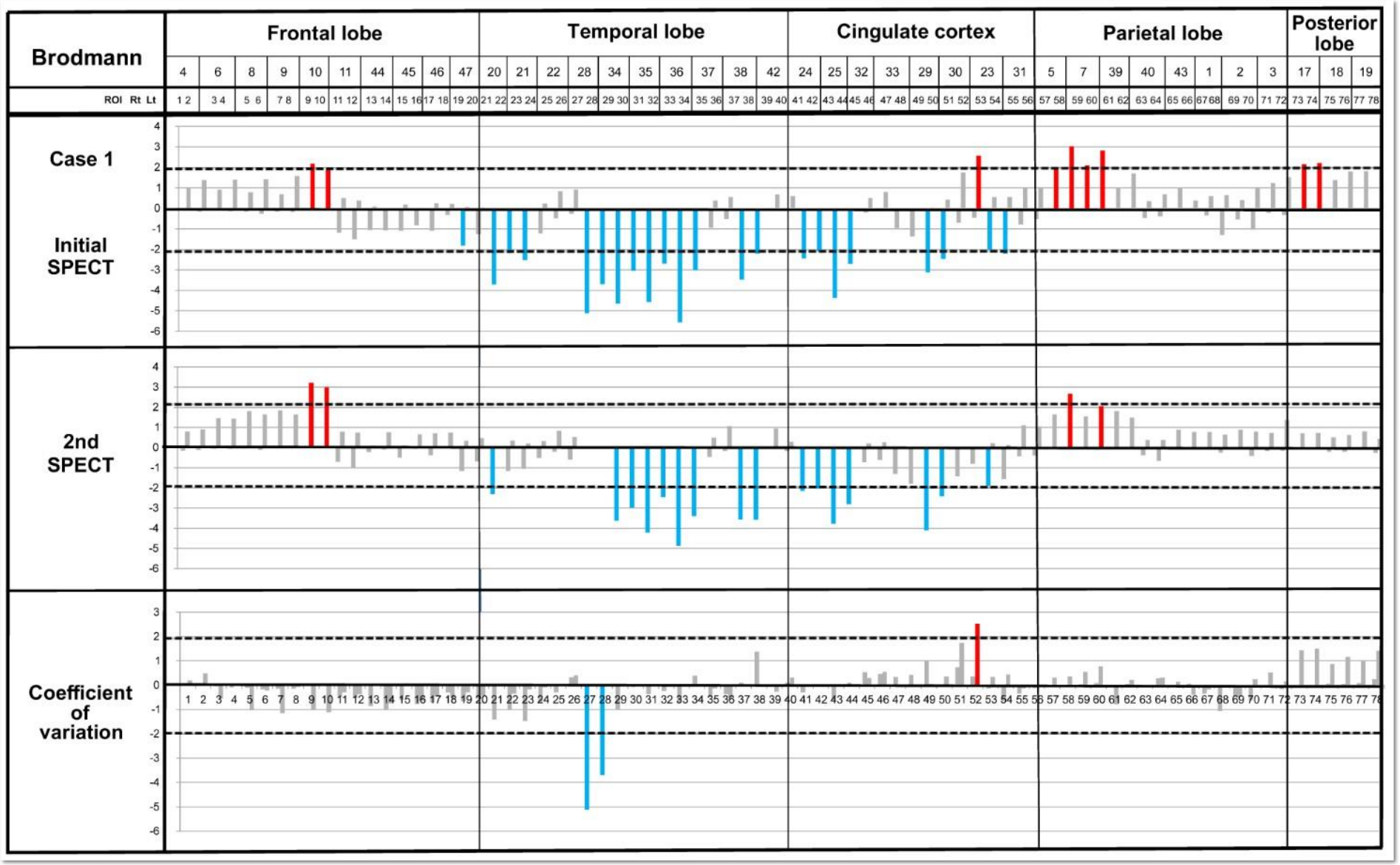
Brodmann
Frontal lobe
Temporal lobe
Cingulate cortex
Parietal lobe
Posterior lobe
4 6 8 9 10 11 44 45 46 47 20 21 22 28 34 35 36 37 38 42 24 25 32 33 29 30 23 31 5 7 39 40 43 1 2 3 17 18 19
ROI Rt Lt
1 2 3 4 5 6 7 8 9 10 11 12 13 14 15 16 17 18 19 20 21 22 23 24 25 26 27 28 29 30 31 32 33 34 35 36 37 38 39 40 41 42 43 44 45 46 47 48 49 50 51 52 53 54 55 56 57 58 59 60 61 62 63 64 65 66 67 68 69 70 71 72 73 74 75 76 77 78
Case 1
Initial SPECT
2nd SPECT
Coefficient of variation

Fig 4. Bar graph showing patients in Groups 1 and 2 according to initial single-photon emission computed tomography. In B30, B31, B7, and B17, the maximum positive iB values were in Group 1 (n = 2). In Group 2, only the right posterior cingulate cortex and Brodmann area 7 were positive.

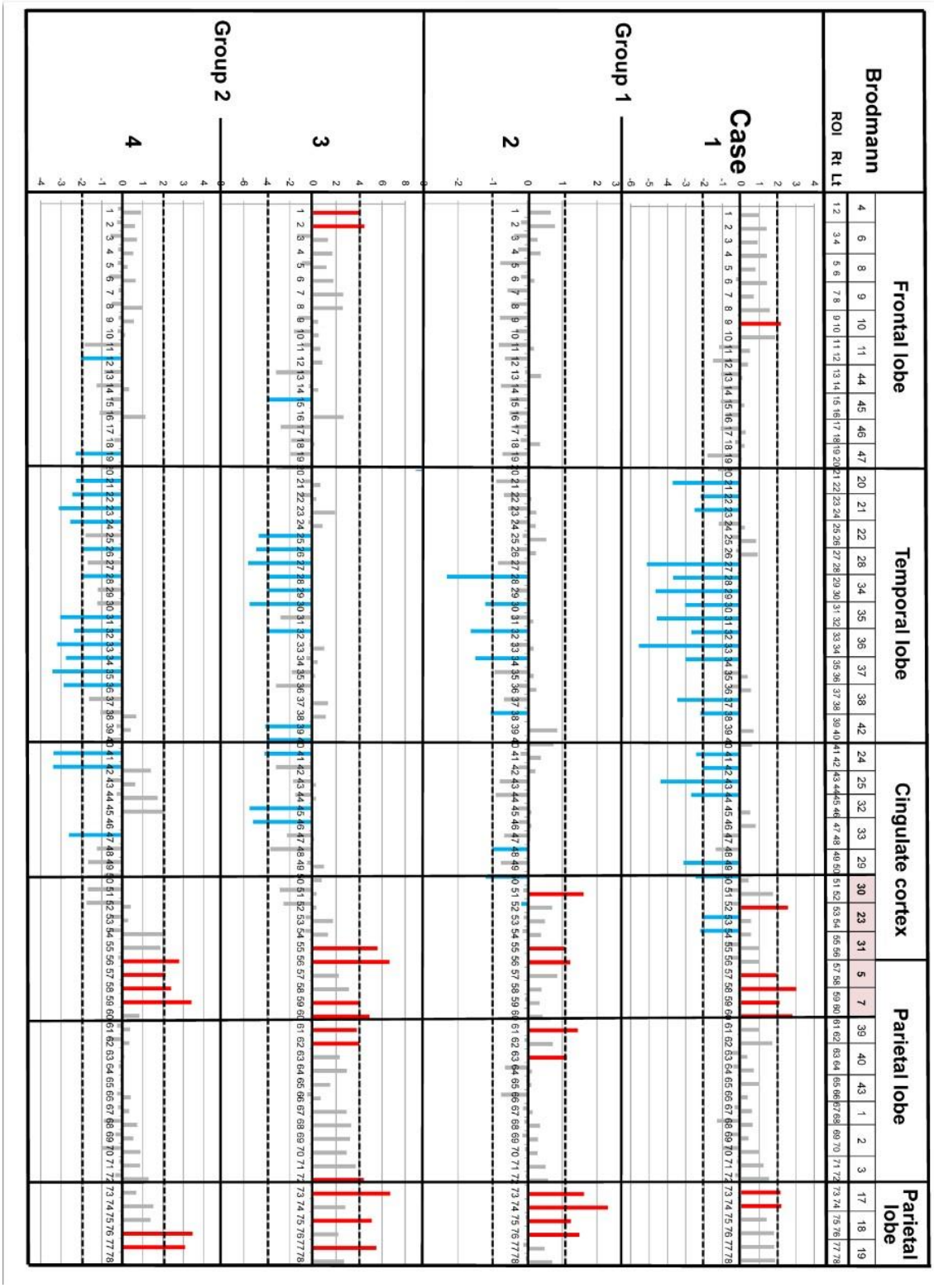

Fig 5. In Group 3, changes common to all regions were negative .

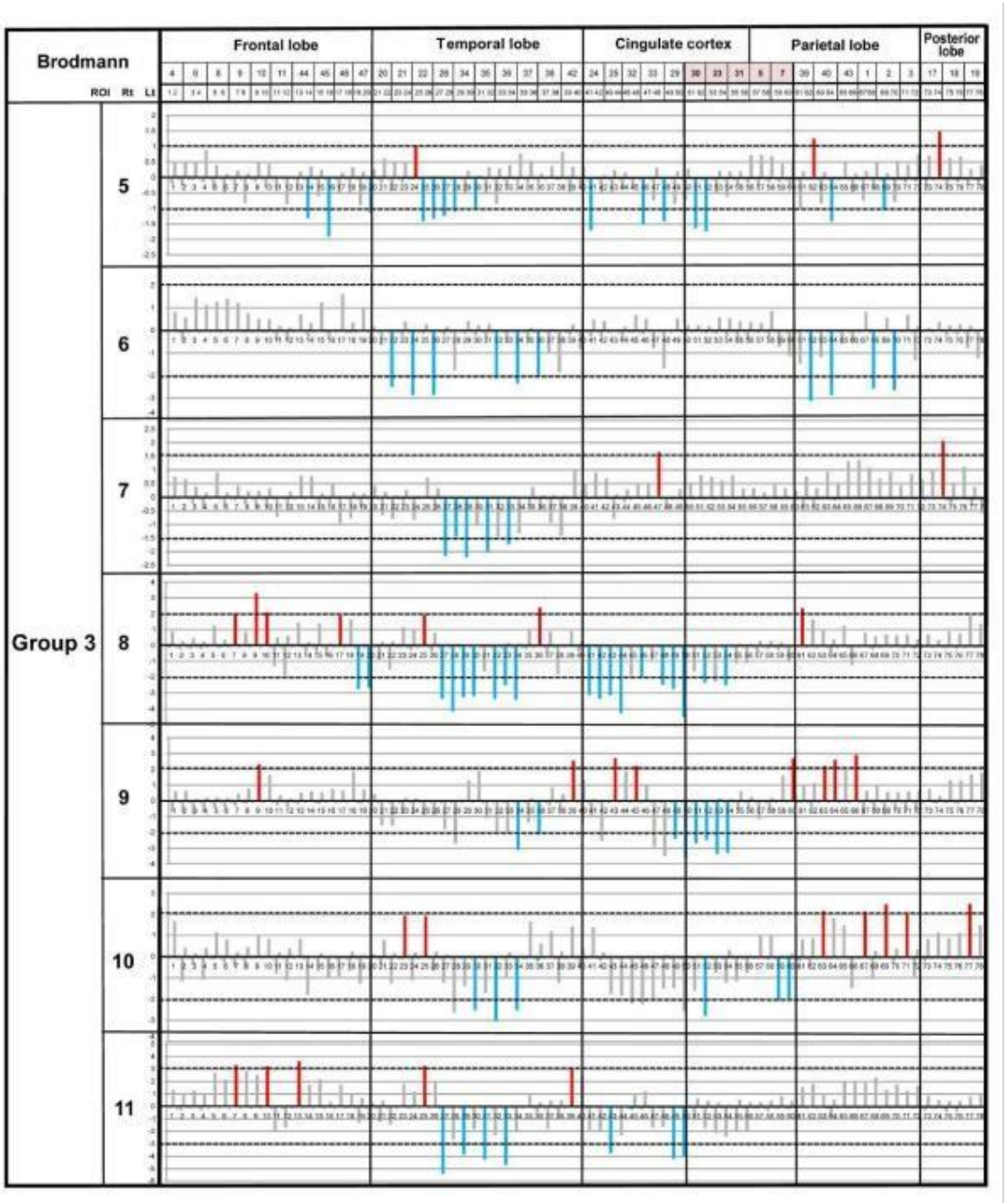

Fig 6. A diagram of the three-dimensional stereotactic surface projection analysis of the retrosplenial cortex/posterior cingulate cortex/Brodmann area 7 for Patients 1–11 arranged for each single-photon emission computed tomography stage. iB30 and B31 increased in Group 1 and decreased or became zero in Group 2. In Group 3, changes were negative. In B7, iB values increased in Groups 1 and 2 and slightly increased or were zero in Group 3.

Transient Global Amnesia